

## Development of a gene-therapy vector for *RDH12*-associated retinal dystrophy

Kecia L. Feathers,<sup>1</sup> Lin Jia,<sup>1</sup> N. Dayanthi Perera,<sup>1</sup> Adrienne Chen,<sup>1</sup> Ferial K. Presswalla,<sup>1</sup> Naheed W. Khan,<sup>1</sup> Abigail T. Fahim,<sup>1</sup> Alexander J. Smith,<sup>3</sup> Robin R. Ali,<sup>1,3</sup> and Debra A. Thompson<sup>1,2,\*</sup>

<sup>1</sup>Department of Ophthalmology and Visual Sciences, and <sup>2</sup>Department of Biological Chemistry, University of Michigan Medical School, Ann Arbor, MI, USA; and <sup>3</sup>Department of Genetics, University College London Institute of Ophthalmology, London EC1V 9EL, UK.

\*To whom correspondence should be addressed: Kellogg Eye Center, 1000 Wall St., Ann Arbor, MI 48105. (734)936-9504. Email: dathom@umich.edu

Short title: Gene therapy for *RDH12* retinal dystrophy

**ABSTRACT**

Early-onset severe retinal degeneration (EOSRD) is a genetically heterogeneous group of diseases resulting in serious visual disability in children. A significant number of EOSRD cases, often diagnosed as Leber congenital amaurosis (LCA13), are associated with mutations in the gene encoding retinol dehydrogenase 12 (RDH12). RDH12 is a member of the enzyme family of short-chain dehydrogenases/reductases. In the retina, RDH12 plays a critical role in reducing toxic retinaldehydes generated by visual cycle activity that is required for the light response of the photoreceptor cells. Individuals with RDH12 deficiency exhibit widespread retinal degeneration impacting both rods and cones. Although *Rdh12*-deficient (*Rdh12*<sup>-/-</sup>) mice do not exhibit retinal degeneration, functional deficits relevant to visual cycle function can be demonstrated. In the present study we describe the development and pre-clinical testing of a recombinant adeno-associated viral (rAAV) vector that has potential for use in treating EOSRD due to *RDH12* mutations. Wild-type and *Rdh12*<sup>-/-</sup> mice that received a sub-retinal injection of rAAV2/5 carrying a human *RDH12* cDNA driven by a human rhodopsin-kinase promoter exhibited transgene expression that was stable, correctly localized, and did not cause retinal toxicity. In addition, administration of the vector reconstituted retinal reductase activity in the retinas of *Rdh12*<sup>-/-</sup> mice, and decreased susceptibility to light damage associated with *Rdh12* deficiency, thus demonstrating potential therapeutic efficacy in an animal model that does not exhibit a retinal degeneration phenotype. These findings support further efforts to develop gene-replacement therapy for individuals with *RDH12* mutations.

## INTRODUCTION

The visual pigments rhodopsin and cone opsins use the vitamin A analog 11-*cis* retinal to absorb light and initiate signaling responses by the photoreceptor cells.<sup>1</sup> Light causes 11-*cis* retinal to isomerize to all-*trans* retinal that stabilizes the signaling conformations of the visual pigments. Following the decay of these species, all-*trans* retinal is released from bleached rhodopsin and cone opsins and recycled to replenish the supply of 11-*cis* retinal chromophore. Although essential for phototransduction, the chemical nature of the vitamin A-dependent visual cycle creates the potential for cellular toxicity. When visual cycle reactions are inefficient or disrupted, retinaldehydes and retinaldehyde-condensation products can accumulate, resulting in damage to the photoreceptor cells and retinal pigment epithelium.<sup>2-4</sup> This can occur as a result of mutations affecting key visual cycle proteins associated with inherited retinal degeneration, or as a result of the cumulative effects of light exposure that may contribute to the pathology of age-related macular degeneration (AMD).<sup>5</sup>

Retinol dehydrogenase 12 (RDH12), also known as short chain dehydrogenase/reductase family 7C member 2, belongs to a family of enzymes that use NADPH to reduce multiple substrates, including 11-*cis* retinaldehyde and all-*trans* retinaldehyde.<sup>6</sup> Although widely expressed outside the eye, in the retina, RDH12 localizes specifically to the inner segments of rod and cone photoreceptor cells.<sup>7,8</sup> Loss-of-function mutations in the gene encoding RDH12 are estimated to cause 3.4%-10.5% of autosomal recessive retinal dystrophy diagnosed as Leber congenital amaurosis (LCA) or early-onset severe retinal dystrophy (EOSRD).<sup>9-12</sup> At young ages, children with RDH12-associated retinal dystrophy exhibit severely decreased visual acuity, visual field constriction, and loss of recordable electroretinogram (ERG) responses, consistent with observed macular atrophy and peripheral pigment accumulation.<sup>11, 13, 14</sup>

Unlike individuals with bi-allelic *RDH12* mutations, *Rdh12*-knockout (*Rdh12*<sup>-/-</sup>) mice exhibit normal retinal histology without apparent retinal degeneration even at advanced ages.<sup>7, 8, 15</sup> Although overall retinoid levels in *Rdh12*<sup>-/-</sup> and wild-type mice are similar, retinal homogenates from the knockout mice have decreased capacity to reduce both all-*trans* retinal and 11-*cis* retinal, and have increased levels of the lipofuscin component A2E.<sup>8</sup> *Rdh12*<sup>-/-</sup> mice also exhibit increased light-damage susceptibility.<sup>7, 16</sup> Thus, despite

the lack of a retinal degeneration phenotype, *Rdh12*<sup>-/-</sup> mice exhibit quantitative measures of RDH12 loss-of-function suitable for use in evaluating therapeutic outcomes, and pertinent to the disease in affected individuals.

Recent advances highlight the promise of adeno-associated virus (AAV)-mediated gene-replacement therapy for the treatment of retinopathies caused by loss-of-function mutations.<sup>17</sup> Studies focused on another visual cycle gene, encoding the retinoid isomerohydrolase RPE65, were the first to show restoration of visual function in affected individuals following sub-retinal administration of AAV2-based vectors carrying *RPE65* cDNA.<sup>18-21</sup> A recombinant AAV2/2-*RPE65* vector, with the trade name Luxturna™, recently became the first FDA-approved gene therapy for an inherited disease.<sup>22</sup> For *RPE65* mutations,<sup>23, 24</sup> vision loss and retinal degeneration result from inability of the RPE to synthesize the chromophore of the visual pigments, 11-*cis* retinal.<sup>25</sup> *RPE65* has served as an exemplary test case for therapeutic strategies designed to restore visual function by increasing chromophore levels, including pharmacologic intervention.<sup>26</sup>

In contrast, loss-of-function mutations affecting genes necessary for the recycling phase of the visual cycle do not decrease chromophore levels, but instead lead to increased levels of toxic retinoid compounds.<sup>27</sup> In the case of mutations in *RDH12*, widespread photoreceptor cell death at young ages likely results from increased exposure to retinaldehydes and short chain aldehydes,<sup>28</sup> due to loss of retinal reductase activity in photoreceptor inner segments.<sup>29</sup> Accordingly, studies of therapeutic intervention in *RDH12*-associated retinal dystrophy have the potential to broadly inform the development of therapeutic strategies to improve the recycling phase of the visual cycle.

To initiate studies of the potential of AAV-mediated gene therapy for *RDH12* loss-of-function, we generated a recombinant AAV2/5 vector carrying human *RDH12* cDNA under the control of a human photoreceptor cell-specific promoter. Conditions were established that achieved stable expression of the *RDH12* transgene that did not result in retinal damage and restored retinal reductase activity in *Rdh12*<sup>-/-</sup> mice. These findings represent an important advance in efforts to establish the feasibility of gene-replacement therapy for inherited retinal degeneration caused by *RDH12* mutations.

## MATERIALS AND METHODS

### rAAV vector construction and purification

Human *RDH12* was amplified from human retinal cDNA by polymerase chain reaction (PCR) using primers designed to encompass the entire *RDH12* coding region, and the product was cloned and sequenced as described previously.<sup>9</sup> The *RDH12* cDNA was inserted into the multiple cloning site of the parental pAAV-hGRK1p.hrGFP vector, and the resulting pAAV-hGRK1p.hRDH12 construct was packaged into AAV. The AAV2/5 pseudotyped vector was generated by bipartite transfection: (1) AAV vector plasmid encoding the gene of interest, (2) AAV helper plasmid encoding AAV Rep proteins from serotype 2 and Cap proteins from serotype 5, and adenovirus helper functions into 293T cells. The transfection and purification were performed using a protocol as published.<sup>30, 31</sup> Two days after transfection, cells were lysed by repeated freeze and thaw cycles. After initial clearing of cell debris, the nucleic acid component of the virus producer cells was removed by Benzonase treatment. The recombinant AAV-vector particles (rAAV2/5-hGRK1p.hRDH12) were purified by affinity chromatography using an AVB Sepharose column (GE Healthcare), washed in 1x PBS and concentrated to a volume of 100–150 ml using Vivaspin 4 (10 kDa) concentrators (Vivaproducts).

Vector titers were determined using quantitative real-time PCR amplification (qPCR).<sup>32</sup> Endotoxin contamination of plasmids, crude vector lysates and purified vectors was measured by Pyrotell-T kinetic turbidimetric assessment (Associates of Cape Cod) following the manufacturer's protocols. Endotoxin levels were below 2.5 EU/mL, which is lower than the US FDA and European Pharmacopoeia specifications per dose.<sup>33</sup> Protein contamination was assessed by SYPRO<sup>TM</sup> Ruby (ThermoFisher) staining of protein blots. A total of  $10^{11}$  viral particles, as determined by qPCR, were run on a 10% polyacrylamide gel together with a reference sample and a size marker, until clear separation between the 75 kDa and 100 kDa bands was achieved. Gels were fixed in 50% methanol and 7% acetic acid for 30 minutes, stained overnight with 0.1% SYPRO<sup>TM</sup> Ruby in fixation solution and washed in 10% methanol and 7% acetic acid for 30 minutes. Proteins were imaged under UV illumination.

## Animals and sub-retinal injections

All experimental procedures complied with the regulations of the University of Michigan Institutional Animal Care and Use Committee (IACUC), and conformed to the guidelines on the care and use of animals adopted by the Association for Research in Vision and Ophthalmology (Rockville, MD, USA). C57BL/6J and BALB/c mice were obtained commercially (The Jackson Laboratory). *Rdh12*<sup>-/-</sup> mice were generated as described previously and bred on mixed C57BL/6J background to generate pigmented animals homozygous for Rpe65-Met<sup>450</sup>, or on a BALB/c background to generate albino animals homozygous for Rpe65-Leu<sup>450</sup>.<sup>15</sup> All mouse strains were confirmed to be Crb1<sup>rd8</sup> negative.<sup>34</sup>

The mice were maintained under cyclic-light conditions (12-hour light-dark, < 20 lux). Young adult mice of both genders in equal numbers were used for injections. Mice were placed under general anesthesia with an intraperitoneal injection of ketamine (80 mg/kg, Par Pharmaceuticals) and xylazine (10 mg/kg, Vet One). Pupils were dilated with topical phenylephrine (2.5%, Paragon BioTek) and tropicamide (1.0%, Akorn). Under an ophthalmic surgical microscope, a small incision was made through the cornea adjacent to the limbus using the tip of a 30-gauge hypodermic needle. A 34-gauge blunt needle fitted to a gas-tight Hamilton syringe was inserted through the incision behind the lens and pushed through the retina. Mice received a sub-retinal injection of 1.3-2  $\mu$ l each to produce bullous retinal detachment in the superior or inferior hemisphere within the nasal quadrant and covering approximately one-third of the retina. The rAAV2/5-hGRK1p.hRDH12 vector, and PBS controls, were administered to one eye of each animal and the other eye was non-injected. For initial optimization, a range of vector concentrations was tested, resulting in doses of  $1.3 \times 10^7$  to  $1.5 \times 10^9$  viral genomes (vg). For analysis of outcomes, the doses used are indicated in the figure legends. Cohorts consisted of 3-8 mice at 5-8 weeks old and studies were performed at least in triplicate. Mice were euthanized by anesthesia overdose by intraperitoneal injection of ketamine (180 mg/kg) and xylazine (20 mg/kg), followed by bilateral pneumothorax.

## Immunohistochemistry and immunoblotting

For immunohistochemistry, mice were euthanized, and eyes were scored for orientation and enucleated. For freeze-substitution<sup>35</sup> processing of rAAV2/5-hGRK1p.hRDH12-injected eyes and controls, whole eyes were flash-frozen in dry-ice-cooled isopentane for 30 seconds, transferred to dry ice-cooled methanol containing 3% glacial acetic acid, incubated at -80°C for 48 h then overnight at -20°C, and embedded in paraffin. Sections (6 µm) were obtained and de-paraffinized, and antigens retrieved in 1mM EDTA, 0.05% Tween 20, pH 8.0, at 90°C for 30 minutes. Sections were permeabilized with PBS plus 0.3% Triton X-100 (PBS-T); blocked with 1% bovine serum albumin, 10% normal goat serum in PBS-T; incubated with primary antibodies overnight at 4°C; then incubated with fluorophore-conjugated secondary antibodies for 1 h at room temperature. Washed sections were cover-slipped using ProLong Gold gel mount containing 4',6-diamidino-2-phenylindole (DAPI; ThermoFisher), and imaged using a Leica DM6000 fluorescence microscope.

For immunoblotting, retinal homogenates were prepared from enucleated eyes in hypotonic lysis buffer containing 0.1% Triton X-100 and protease inhibitors, then subjected to SDS-polyacrylamide electrophoresis and transferred onto nitrocellulose. The membranes were blocked, incubated with primary antibody overnight, washed, incubated with alkaline phosphatase-conjugated secondary antibody, washed, and developed using 5-bromo-4-chloro-3'-indolyphosphate p-toluidine and nitro-blue tetrazolium chloride (Sigma).

Primary antibodies used were: a mouse anti-RDH12 monoclonal (2C9) specific for the human protein;<sup>15</sup> a rabbit anti-Rdh12 polyclonal (CSP) specific for the mouse protein;<sup>15</sup> a mouse anti-RHO monoclonal (1D4);<sup>36</sup> a rabbit anti-RHO polyclonal;<sup>37</sup> a rabbit anti-red/green cone opsin polyclonal (Millipore); and a mouse anti-GAPDH monoclonal (ThermoFisher).

## Optical Coherence Tomography

Mice were anesthetized and pupils dilated as described for sub-retinal injections. Systane lubricant eye drops (Alcon) were given for corneal hydration. Optical coherence tomography (OCT) was performed with a spectral domain optical coherence tomography

system (Bioptigen Envisu R2200 SD-OCT system). The camera lens was adjusted to acquire images from eyes without physical contact. A volume analysis centered on the optic nerve head was performed. The volume size was 1.4 x 1.4 mm.

### Quantification of retinoid content

Levels of all-*trans* retinal and 11-*cis* retinal in mouse eyes were determined as described previously.<sup>15</sup> In brief, mice at 6 weeks postinjection were dark-adapted overnight, transferred to dim red light, euthanized via anesthesia overdose, and the eyes were enucleated and frozen in liquid N<sub>2</sub>. Each eye was homogenized in 1 mL chloroform:methanol:hydroxylamine (2 M) (3:6:1) on ice, sonicated with a microtip probe (30 times for 1 second) on ice, then incubated at room temperature for 2 minutes. Chloroform (200 µL) and water (240 µL) were added and mixed by vortexing, and the phases separated by centrifugation. The lower phases were collected, dried under argon, and dissolved in hexane. Retinoids were identified and quantified by normal-phase high-performance liquid chromatography (HPLC) using a Waters Alliance separation module and photodiode array detector with a Supelcosil LC-31 column (25 cm by 4.6 mm by 3 µm) developed with 5% 1,4-dioxane in hexane. Peaks were identified by comparison to retention times of standard compounds and evaluation of wavelength maxima, and quantified by comparison of peak areas at 347 and 351 nm for *syn* and *anti* 11-*cis* retinal oxime, respectively (generated from 11-*cis* retinal (National Eye Institute)), and at 357 and 361 nm for *syn* and *anti* all-*trans* retinal oxime, respectively (generated from all-*trans* retinal (Sigma)).

### Retinal reductase assays

Mouse retina homogenates were assayed for retinal reductase activity at 6 weeks postinjection, as described previously.<sup>8</sup> Briefly, light-adapted mice were euthanized, eyes enucleated, and each dissected retina was homogenized individually in 125 µl of 0.25 M sucrose, 25 mM Tris-acetate, pH 7, 1 mM dithiothreitol. The homogenates were centrifuged at 1000 × *g* for 5 minutes to remove unbroken cells, and the supernates were sonicated with a microtip probe (30 times for 1 second) on ice. Protein concentrations were determined by a modification of the Lowry procedure,<sup>38</sup> and RDH12 expression was evaluated by western analysis. Like samples were pooled from 3-5 mice, and 20 µg of each pooled lysate was assayed in triplicate in buffer containing 200 µM all-*trans* retinal and 200 µM NADPH in HEPES buffer (pH 7). Reactions were incubated for 0–45 minutes at 37°C,

and retinoids were extracted in chloroform-methanol. All-*trans*-retinol formation was quantitated using normal-phase HPLC analysis with comparison to standards (Sigma), as described above.

### **Electroretinogram (ERG) recordings**

ERG analysis was performed as described previously using the Espion e2 recording system (Diagnosys).<sup>39</sup> In brief, mice were anesthetized and pupils dilated as described for sub-retinal injections. Body temperature was maintained at 37°C with a heating pad. Corneal ERGs were recorded from both eyes using gold wire loops with 0.5% tetracaine topical anesthesia and a drop of 2% methylcellulose for corneal hydration. A gold wire loop placed in the mouth was used as reference, and a ground electrode was on the tail. The ERG protocol consisted of recording dark-adapted (scotopic) responses to brief white flashes ( $-2.31 \log \text{ cd.s.m}^{-2}$  for rod isolated B-waves;  $1.09 \log \text{ cd.s.m}^{-2}$  for rod-cone combined response). Light-adapted (photopic) ERGs were recorded after 10 minutes of adaptation to a white  $32 \text{ cd.m}^{-2}$  rod-suppressing background in response to  $1.09 \log \text{ cd.s.m}^{-2}$  intensity flashes. Responses were amplified at 1,000 gain at 1.25 to 1000 Hz, and digitized at a rate of 2000 Hz. A notch filter was used to remove 60 Hz line noise. Responses were computer-averaged and recorded at 3- to 60-second intervals depending upon the stimulus intensity.

### **Light-induced retinal damage**

Mice received a sub-retinal injection of rAAV2/5-hGRK1p.hRDH12, or an equal volume of PBS, and contralateral eyes were not injected. Beginning 6 weeks later, ERG analysis was performed and scotopic responses were quantified as described above. The following week, mice were dark-adapted overnight, their pupils dilated with tropicamide (1.0%), and then were placed in a light-box in individual clear trays. The mice were exposed to 5,000 lux for 2 hours, and then were returned to vivarium housing (12 hour light-dark) for 7 days, after which ERG analysis was repeated. The percent ERG response remaining after light damage was calculated for each eye, and the averages for each cohort were calculated.

### **Statistical analysis**

Graphed data show mean values  $\pm$  standard error of the mean (GraphPad, Prism). For analysis of retinoid content, after performing D'Agostino-Pearson omnibus normality

test and Bartlett's test for equal variance, comparison among multiple groups was made using one-way analysis of variance. For analysis of RDH activity, after subjecting the data to F-test to determine the appropriate t-test parameters, comparison of initial rates was made using two-tailed t-tests. For analysis of ERG amplitudes, comparison of the responses in treated eyes and untreated eyes was made using two-tailed paired t-tests. In all tests, significance is indicated as:  $p < 0.05$ , \*;  $p < 0.01$ , \*\*;  $p < 0.001$ , \*\*\*.

## RESULTS

### rAAV2/5-mediated expression of human RDH12 in mouse photoreceptors

Our efforts to develop an RDH12 gene-therapy vector focused on the use of AAV2 pseudotyped with AAV5 capsids (AAV2/5), as vectors of the AAV5 serotype have previously been shown to mediate efficient transduction of photoreceptor cells in the murine and primate retina.<sup>40, 41</sup> A human *RDH12* cDNA was cloned into an AAV2 construct downstream of a human rhodopsin kinase (GRK1) promoter that drives photoreceptor-specific expression (**Fig. 1A**).<sup>42-44</sup> After packaging with AAV5 capsid, the rAAV2/5-hGRK1p.hRDH12 vector was produced in transduced cells, purified, and assessed on protein gels (**Fig. 1B**). Wild-type (C57BL/6J) and *Rdh12*<sup>-/-</sup> (knockout) mice at 5-8 weeks of age received a sub-retinal injection of rAAV2/5-hGRK1p.hRDH12 at a range of doses ( $1.3 \times 10^7$  to  $1.5 \times 10^9$  vg). At 6 weeks postinjection of  $1.4$ - $1.5 \times 10^9$  vg, western blots of retinal proteins using an antibody specific for human RDH12 (2C9) showed stable expression of the recombinant protein in injected *Rdh12*<sup>-/-</sup> mice, whereas an antibody specific for mouse *Rdh12* (CSP) detected the endogenous mouse protein in non-injected wild-type mice (**Fig. 1C**). In mice that received the same dose of rAAV2/5-hGRK1p.hRDH12, immunohistochemical analysis of human RDH12 expression showed co-localization with endogenous mouse *Rdh12* in photoreceptor inner segments in injected wild-type mice, and a similar pattern of expression in injected *Rdh12*<sup>-/-</sup> mice (**Fig. 1D**).

OCT analysis of mice that received a sub-retinal injection of rAAV2/5-hGRK1p.hRDH12 showed minor injection site scarring, but no significant alterations in laminar structure across a distance of 1,000  $\mu\text{m}$  on both sides of the optic nerve head (**Fig. 2A**). Immunohistochemical analysis of rhodopsin and red/green opsin showed no evidence of mislocalization or decreased expression indicative of photoreceptor toxicity. Co-staining confirmed their correct localization relative to RDH12 in both rod and cone

photoreceptor cells of wild-type and *Rdh12*<sup>-/-</sup> mice that received a sub-retinal injection of rAAV2/5-hGRK1p.hRDH12 (**Fig. 2B**).

### **rAAV2/5-mediated expression of human RDH12 restores retinal reductase activity in *Rdh12*<sup>-/-</sup> mouse retinas**

Although *Rdh12*<sup>-/-</sup> mice do not exhibit a retinal degeneration phenotype, the ability of their retinas to reduce exogenous retinaldehydes is significantly decreased,<sup>8</sup> with residual activity attributed to the presence of other RDH isoforms.<sup>6, 45</sup> To assay the retinal reductase activity in mice that received a sub-retinal injection of rAAV2/5-hGRK1p.hRDH12, relative to that in controls, retinal homogenates were assayed using HPLC analysis to quantitate the conversion of exogenous all-*trans* retinal to all-*trans* retinol (**Fig. 3A**). Retinas from *Rdh12*<sup>-/-</sup> mice that received a sub-retinal injection of rAAV2/5-hGRK1p.hRDH12 (1.4 x 10<sup>9</sup> vg) exhibited an average initial rate of all-*trans* retinol formation of 0.046 pmol min<sup>-1</sup> μg protein<sup>-1</sup>, which was significantly increased relative to the average for non-injected *Rdh12*<sup>-/-</sup> mice (0.013 pmol min<sup>-1</sup> μg protein<sup>-1</sup>), and PBS-injected *Rdh12*<sup>-/-</sup> mice (0.016 pmol min<sup>-1</sup> μg protein<sup>-1</sup>) (p < 0.01). The average initial rate of all-*trans* retinol formation in non-injected wild-type control mice was 0.071 pmol min<sup>-1</sup> μg protein<sup>-1</sup>. Since the injection bleb covered an estimated one-fourth to one-third of the retina (**Fig. 3B**), we estimate the level of the recombinant human protein in the treated area of retina to be, on average, approximately twice that of the endogenous mouse protein.

### **rAAV2/5-mediated expression of human RDH12 does not significantly reduce chromophore levels in *Rdh12*<sup>-/-</sup> mouse retinas**

The capacity of RDH12 to reduce both all-*trans* retinal and the chromophore 11-*cis* retinal suggests that over expression or mislocalization of human RDH12 has the potential to negatively impact visual cycle function. HPLC analysis of retinoid content was used to evaluate visual-cycle function in *Rdh12*<sup>-/-</sup> mice that received a sub-retinal injection of rAAV2/5-hGRK1p.hRDH12 (1.4 x 10<sup>9</sup> vg), as well as in PBS-injected and non-injected wild-type controls (**Fig. 4A**). The levels of 11-*cis* retinal (mean ± std. error) in retinas of non-injected wild-type mice, and *Rdh12*<sup>-/-</sup> mice from each treatment group, were not significantly different (C57BL/6J, 547 ± 11 pmol/eye; *Rdh12*<sup>-/-</sup> non-injected, 503 ± 29 pmol/eye; *Rdh12*<sup>-/-</sup> rAAV2/5-hGRK1p. hRDH12-injected, 453 ± 16 pmol/eye; *Rdh12*<sup>-/-</sup> PBS-

injected,  $455 \pm 26$  pmol/eye) ( $p > 0.05$ ) (**Fig. 4B**). In contrast, the levels of all-*trans* retinal were significantly decreased only in vector injected *Rdh12*<sup>-/-</sup> mice (C57BL/6J,  $30 \pm 5$  pmol/eye; *Rdh12*<sup>-/-</sup> non-injected,  $44 \pm 5$  pmol/eye; *Rdh12*<sup>-/-</sup> rAAV2/5-hGRK1p.hRDH12-injected,  $29 \pm 4$  pmol/eye; *Rdh12*<sup>-/-</sup> PBS-injected ( $36 \pm 4$  pmol/eye) ( $p < 0.05$ ) (**Fig. 4C**). Taken together, these findings show no evidence of visual cycle disruption resulting from rAAV2/5-hGRK1p.hRDH12-mediated expression of human RDH12 in mice, and instead document a modest decrease in all-*trans* retinal potentially consistent with an *in vivo* therapeutic effect.

### Visual function is maintained in mice expressing human RDH12

Electroretinography (ERG) of retinal electrical activity elicited by light stimuli of varying intensities was used to evaluate retinal function in wild-type and *Rdh12*<sup>-/-</sup> mice at various times after a sub-retinal injection of rAAV2/5-hGRK1p.hRDH12 ( $1.4 \times 10^9$  vg) or PBS. Analysis of scotopic and photopic ERG responses showed that expression of human RDH12 did not result in significant decreases in rod or cone function relative to non-injected eyes at 6 weeks postinjection (**Fig. 5**). Small decreases in ERG amplitudes detected in both wild-type and *Rdh12*<sup>-/-</sup> mice at 6 weeks postinjection are likely due to the effects of retinal detachment. At times up to 54 weeks postinjection there were no significant differences in ERG magnitudes between non-injected and rAAV2/5-hGRK1p.hRDH12-injected eyes of wild-type mice, or between non-injected and rAAV2/5-hGRK1p.hRDH12-injected eyes of *Rdh12*<sup>-/-</sup> mice, as determined by pair-wise comparisons ( $p > 0.10$ ) (**Suppl. Fig. 1**). A decrease in ERG amplitudes over time was observed in all mice, reflecting the consequences of aging. Both wild-type and *Rdh12*<sup>-/-</sup> mice that received a sub-retinal injection of rAAV2/5-hGRK1p.hRDH12 exhibited robust transgene expression and preserved retinal structure at 54 weeks postinjection (**Suppl. Fig. 2A**), with no evidence of mislocalization of rod and cone opsins indicative of photoreceptor cell death (**Suppl. Fig. 2B**). OCT analysis at 54 weeks postinjection showed good preservation of retinal microstructure (**Suppl. Fig. 2C**).

### Human RDH12 protects against light damage in *Rdh12*<sup>-/-</sup> mice

Previous studies have shown that *Rdh12*<sup>-/-</sup> mice exhibit increased susceptibility to light damage.<sup>7</sup> Increased light damage resulting from RDH12 deficiency is likely to be specifically linked to increased retinaldehydes and other short-chain aldehydes.<sup>16, 29</sup> It is

also known that a polymorphism in the mouse gene encoding Rpe65, the retinoid isomerohydrolase that generates 11-*cis* retinal, is a determining factor in susceptibility to light damage, which is greater in mice homozygous for leucine at amino acid residue 450 (Rpe65-Leu450) than in mice homozygous for methionine (Rpe65-Met450).<sup>46</sup> For studies of light-damage susceptibility, *Rdh12*<sup>-/-</sup> mice were bred onto the albino BALB/c background to generate knockout mice homozygous for Rpe65-Leu450. BALB/c and albino *Rdh12*<sup>-/-</sup> mice received a sub-retinal injection of rAAV2/5-hGRK1p.hRDH12 ( $1.4 \times 10^9$  vg) in one eye, and received no treatment in the contralateral eye. At 6 weeks postinjection, ERG analysis of retinal activity was performed 1 week before, and 1 week after, subjecting the mice to light levels that cause significant retinal damage in the albino animals (5,000 lux for 2 h). Under photopic conditions, B-wave amplitudes obtained after light damage were variable for both BALB/c and albino *Rdh12*<sup>-/-</sup> mice. In contrast, under scotopic conditions, the percent of rod-isolated and combined rod-cone activity remaining in eyes of albino *Rdh12*<sup>-/-</sup> mice that received a sub-retinal injection of rAAV2/5-hGRK1p.hRDH12 was significantly greater than that remaining in untreated eyes ( $p \leq 0.001$ ) (**Figure 6**). In addition, the eyes of BALB/c mice that received a sub-retinal injection of rAAV2/5-hGRK1p.hRDH12 did not exhibit significantly greater activity than that remaining in untreated eyes ( $p \geq 0.2275$ ). The very high level of significance obtained in pairwise comparisons of rod and rod-cone function remaining in treated and untreated *Rdh12*<sup>-/-</sup> mice provides strong evidence of a protective role of rAAV2/5-hGRK1p.hRDH12 in reducing light-damage susceptibility associated with RDH12 deficiency.

## DISCUSSION

Multiple factors identify *RDH12*-associated retinal dystrophy as a compelling target for gene therapy, including its autosomal recessive mode of inheritance, prevalence in early-onset disease, severe disease burden, and effect on a well-defined biological pathway. However, a significant challenge for establishing therapeutic efficacy in pre-clinical studies is the absence of a retinal degeneration phenotype in *Rdh12*<sup>-/-</sup> mice that is similar to that caused by *RDH12* mutations in patients. Thus our studies were designed to evaluate functional outcome measures that directly reflect the activity of the *RDH12* transgene. Administration of rAAV2/5-hGRK1p.hRDH12 to *Rdh12*<sup>-/-</sup> mice by sub-retinal injection was shown to result in stable expression of RDH12 that localizes to the photoreceptor cells,

reconstitutes *in vivo* retinal reductase activity, and decreases light-damage sensitivity. These findings provide strong support for the potential of gene supplementation to reconstitute RDH12 function in photoreceptor cells and decrease retinal degeneration in individuals with EOSRD due to *RDH12*-mutations.

As a member of the family of short-chain dehydrogenases/reductases, RDH12 exhibits broad substrate specificity that includes both 11-*cis* and all-*trans* retinaldehydes, as well as lipid peroxidation products.<sup>6, 16</sup> It follows that RDH12 over expression and/or mislocalization has the potential to disrupt photoreceptor cell homeostasis, in part, by skewing the retinol-retinaldehyde balance needed to maintain visual cycle function and photopigment stability. Notably, our studies in wild-type and *Rdh12*<sup>-/-</sup> mice treated by sub-retinal injection of rAAV2/5-hGRK1p.hRDH12 and evaluated over the course of at least one year using multiple forms of analysis showed no evidence of retinal damage or disruptions in retinoid metabolism. These findings identify rAAV2/5-hGRK1p.hRDH12 as a strong therapeutic candidate, and represent a significant advance in the progress needed to move toward a Phase I/II clinical trial.

Although the disease associated with *RDH12* mutations results in early and severe retinal degeneration, recent natural history studies suggest that a therapeutic window of opportunity may exist for many patients. Despite that fact that ERG responses are extinguished at young ages, areas of preserved photoreceptors in the peripheral retina, observed by fundus exam and OCT,<sup>12, 47</sup> likely contribute to visual function retained into adolescence, and in a few cases, to relatively older ages. A logical strategy would be to target these areas in an effort to decrease the rate of cell death and delay or prevent further loss of peripheral vision. Macular atrophy is an early finding in nearly all patients,<sup>10-13, 48, 49</sup> documented as young as 3 years of age, although some children retain areas of preserved ONL and ellipsoid in the macula on OCT.<sup>12, 47, 50, 51</sup> Preservation of useful central vision may be possible with early childhood intervention, using OCT as a guide. Thus, there is a critical need for early-stage patient identification through genetic screening, for which patient registries are likely to play an important role.

With the identification of rAAV2/5-hGRK1p.hRDH12 as a strong therapeutic candidate, coupled with advances occurring in patient identification and characterization,

the realization of a Phase I/II clinical trial of *RDH12* gene-replacement therapy may be close at hand.

### **ACKNOWLEDGMENTS**

This study was supported by Foundation Fighting Blindness, RDH12 Fund for Sight, Research to Prevent Blindness (chair award), University of Michigan Kellogg Eye Center, NIH Core Grant for Vision Research (P30 EY-07003), Medical Research Council grant MR/J005215/1, the NIHR Biomedical Research Centre based at Moorfields Eye Hospital, NHS Foundation Trust, University College London Institute of Ophthalmology, and RP Fighting Blindness.

### **AUTHOR DISCLOSURES**

DAT, AJS, and RRA are inventors on a pending patent application on *RDH12*-gene therapy that has been filed by the University of Michigan and University College London; AJS and RRA have financial interests in MeiraGTx PLC; KLF, no competing financial interests exist; LJ, no competing financial interests exist; NDP, no competing financial interests exist; AC, no competing financial interests exist; FKP, no competing financial interests exist; NWK, no competing financial interests exist; ATF, no competing financial interests exist.

## LITERATURE CITED

1. Palczewski K. Chemistry and biology of vision. *J Biol Chem* 2012;287:1612-1619.
2. Ben-Shabat S, Parish CA, Hashimoto M, Liu J, Nakanishi K, Sparrow JR. Fluorescent pigments of the retinal pigment epithelium and age-related macular degeneration. *Bioorg Med Chem Lett* 2001;11:1533-1540.
3. Sparrow JR, Hicks D, Hamel CP. The retinal pigment epithelium in health and disease. *Current molecular medicine* 2010;10:802-823.
4. Travis GH, Golczak M, Moise AR, Palczewski K. Diseases caused by defects in the visual cycle: retinoids as potential therapeutic agents. *Annu Rev Pharmacol Toxicol* 2007;47:469-512.
5. Sparrow JR, Gregory-Roberts E, Yamamoto K, et al. The bisretinoids of retinal pigment epithelium. *Prog Retin Eye Res* 2012;31:121-135.
6. Haeseleer F, Jang GF, Imanishi Y, et al. Dual-substrate specificity short chain retinol dehydrogenases from the vertebrate retina. *J Biol Chem* 2002;277:45537-45546.
7. Maeda A, Maeda T, Imanishi Y, et al. Retinol dehydrogenase (RDH12) protects photoreceptors from light-induced degeneration in mice. *J Biol Chem* 2006;281:37697-37704.
8. Chrispell JD, Feathers KL, Kane MA, et al. Rdh12 activity and effects on retinoid processing in the murine retina. *J Biol Chem* 2009;284:21468-21477.
9. Janecke AR, Thompson DA, Utermann G, et al. Mutations in RDH12 encoding a photoreceptor cell retinol dehydrogenase cause childhood-onset severe retinal dystrophy. *Nat Genet* 2004;36:850-854.
10. Perrault I, Hanein S, Gerber S, et al. Retinal dehydrogenase 12 (RDH12) mutations in leber congenital amaurosis. *Am J Hum Genet* 2004;75:639-646.
11. Mackay DS, Dev Borman A, Moradi P, et al. RDH12 retinopathy: novel mutations and phenotypic description. *Mol Vis* 2011;17:2706-2716.
12. Zou X, Fu Q, Fang S, et al. Phenotypic Variability of Recessive Rdh12-Associated Retinal Dystrophy. *Retina* 2018.
13. Schuster A, Janecke AR, Wilke R, et al. The phenotype of early-onset retinal degeneration in persons with RDH12 mutations. *Invest Ophthalmol Vis Sci* 2007;48:1824-1831.

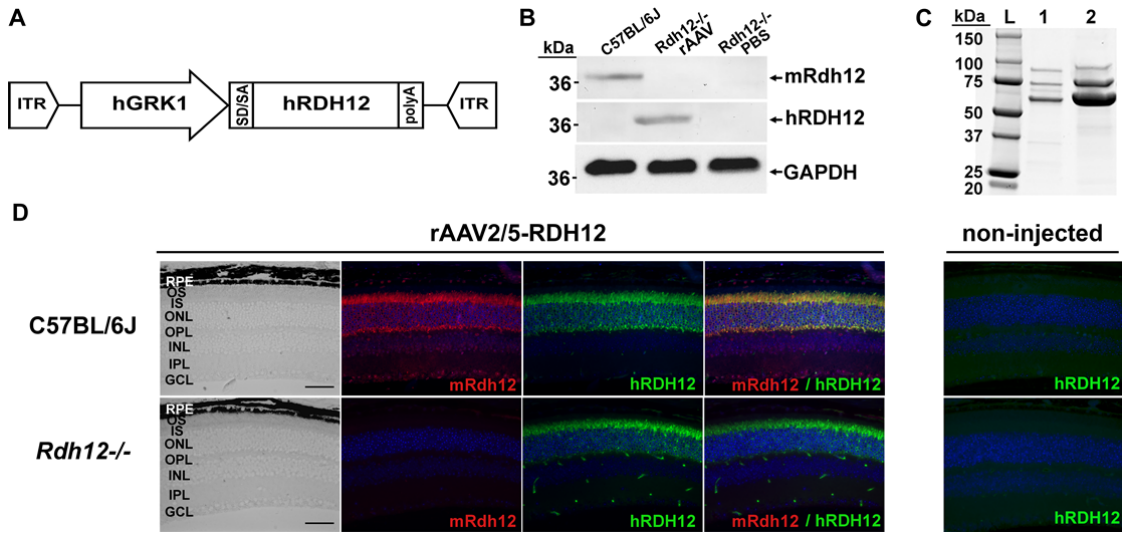
14. Jacobson SG, Cideciyan AV, Aleman TS, et al. RDH12 and RPE65, visual cycle genes causing leber congenital amaurosis, differ in disease expression. *Invest Ophthalmol Vis Sci* 2007;48:332-338.
15. Kurth I, Thompson DA, Ruther K, et al. Targeted disruption of the murine retinal dehydrogenase gene *Rdh12* does not limit visual cycle function. *Mol Cell Biol* 2007;27:1370-1379.
16. Marchette LD, Thompson DA, Kravtsova M, Ngansop TN, Mandal MN, Kasus-Jacobi A. Retinol dehydrogenase 12 detoxifies 4-hydroxynonenal in photoreceptor cells. *Free Radic Biol Med* 2010;48:16-25.
17. Boye SE, Boye SL, Lewin AS, Hauswirth WW. A comprehensive review of retinal gene therapy. *Mol Ther* 2013;21:509-519.
18. Bainbridge JW, Smith AJ, Barker SS, et al. Effect of gene therapy on visual function in Leber's congenital amaurosis. *N Engl J Med* 2008;358:2231-2239.
19. Maguire AM, Simonelli F, Pierce EA, et al. Safety and efficacy of gene transfer for Leber's congenital amaurosis. *N Engl J Med* 2008;358:2240-2248.
20. Cideciyan AV, Aleman TS, Boye SL, et al. Human gene therapy for RPE65 isomerase deficiency activates the retinoid cycle of vision but with slow rod kinetics. *Proc Natl Acad Sci U S A* 2008;105:15112-15117.
21. Hauswirth WW, Aleman TS, Kaushal S, et al. Treatment of leber congenital amaurosis due to RPE65 mutations by ocular subretinal injection of adeno-associated virus gene vector: short-term results of a phase I trial. *Hum Gene Ther* 2008;19:979-990.
22. Ameri H. Prospect of retinal gene therapy following commercialization of voretigene neparvovec-rzyl for retinal dystrophy mediated by RPE65 mutation. *Journal of current ophthalmology* 2018;30:1-2.
23. Gu SM, Thompson DA, Srikumari CR, et al. Mutations in RPE65 cause autosomal recessive childhood-onset severe retinal dystrophy. *Nat Genet* 1997;17:194-197.
24. Marlhens F, Bareil C, Griffoin JM, et al. Mutations in RPE65 cause Leber's congenital amaurosis. *Nat Genet* 1997;17:139-141.
25. Redmond TM, Yu S, Lee E, et al. Rpe65 is necessary for production of 11-cis-vitamin A in the retinal visual cycle. *Nat Genet* 1998;20:344-351.

26. Koenekoop RK, Sui R, Sallum J, et al. Oral 9-cis retinoid for childhood blindness due to Leber congenital amaurosis caused by RPE65 or LRAT mutations: an open-label phase 1b trial. *Lancet* 2014.
27. Saari JC. Vitamin A and Vision. *Sub-cellular biochemistry* 2016;81:231-259.
28. Belyaeva OV, Korkina OV, Stetsenko AV, Kim T, Nelson PS, Kedishvili NY. Biochemical properties of purified human retinol dehydrogenase 12 (RDH12): catalytic efficiency toward retinoids and C9 aldehydes and effects of cellular retinol-binding protein type I (CRBPI) and cellular retinaldehyde-binding protein (CRALBP) on the oxidation and reduction of retinoids. *Biochemistry* 2005;44:7035-7047.
29. Chen C, Thompson DA, Koutalos Y. Reduction of all-trans-retinal in vertebrate rod photoreceptors requires the combined action of RDH8 and RDH12. *J Biol Chem* 2012;287:24662-24670.
30. Nishiguchi KM, Carvalho LS, Rizzi M, et al. Gene therapy restores vision in rd1 mice after removal of a confounding mutation in Gpr179. *Nature communications* 2015;6:6006.
31. Georgiadis A, Duran Y, Ribeiro J, et al. Development of an optimized AAV2/5 gene therapy vector for Leber congenital amaurosis owing to defects in RPE65. *Gene Ther* 2016;23:857-862.
32. Aurnhammer C, Haase M, Muether N, et al. Universal real-time PCR for the detection and quantification of adeno-associated virus serotype 2-derived inverted terminal repeat sequences. *Human gene therapy methods* 2012;23:18-28.
33. Penaud-Budloo M, Francois A, Clement N, Ayuso E. Pharmacology of Recombinant Adeno-associated Virus Production. *Molecular therapy Methods & clinical development* 2018;8:166-180.
34. Mattapallil MJ, Wawrousek EF, Chan CC, et al. The Rd8 mutation of the Crb1 gene is present in vendor lines of C57BL/6N mice and embryonic stem cells, and confounds ocular induced mutant phenotypes. *Invest Ophthalmol Vis Sci* 2012;53:2921-2927.
35. Sun N, Shibata B, Hess JF, FitzGerald PG. An alternative means of retaining ocular structure and improving immunoreactivity for light microscopy studies. *Mol Vis* 2015;21:428-442.

36. MacKenzie D, Arendt A, Hargrave P, McDowell JH, Molday RS. Localization of binding sites for carboxyl terminal specific anti-rhodopsin monoclonal antibodies using synthetic peptides. *Biochemistry* 1984;23:6544-6549.
37. Khorana HG, Knox BE, Nasi E, Swanson R, Thompson DA. Expression of a bovine rhodopsin gene in *Xenopus* oocytes: demonstration of light-dependent ionic currents. *Proc Natl Acad Sci U S A* 1988;85:7917-7921.
38. Peterson GL. A simplification of the protein assay method of Lowry et al. which is more generally applicable. *Anal Biochem* 1977;83:346-356.
39. Thompson DA, Khan NW, Othman MI, et al. Rd9 is a naturally occurring mouse model of a common form of retinitis pigmentosa caused by mutations in RPGR-ORF15. *PLoS One* 2012;7:e35865.
40. Yang GS, Schmidt M, Yan Z, et al. Virus-mediated transduction of murine retina with adeno-associated virus: effects of viral capsid and genome size. *J Virol* 2002;76:7651-7660.
41. Lotery AJ, Yang GS, Mullins RF, et al. Adeno-associated virus type 5: transduction efficiency and cell-type specificity in the primate retina. *Hum Gene Ther* 2003;14:1663-1671.
42. Khani SC, Pawlyk BS, Bulgakov OV, et al. AAV-mediated expression targeting of rod and cone photoreceptors with a human rhodopsin kinase promoter. *Invest Ophthalmol Vis Sci* 2007;48:3954-3961.
43. Sun X, Pawlyk B, Xu X, et al. Gene therapy with a promoter targeting both rods and cones rescues retinal degeneration caused by AIPL1 mutations. *Gene Ther* 2010;17:117-131.
44. Mihelec M, Pearson RA, Robbie SJ, et al. Long-term preservation of cones and improvement in visual function following gene therapy in a mouse model of leber congenital amaurosis caused by guanylate cyclase-1 deficiency. *Hum Gene Ther* 2011;22:1179-1190.
45. Rattner A, Smallwood PM, Nathans J. Identification and characterization of all-trans-retinol dehydrogenase from photoreceptor outer segments, the visual cycle enzyme that reduces all-trans-retinal to all-trans-retinol. *J Biol Chem* 2000;275:11034-11043.

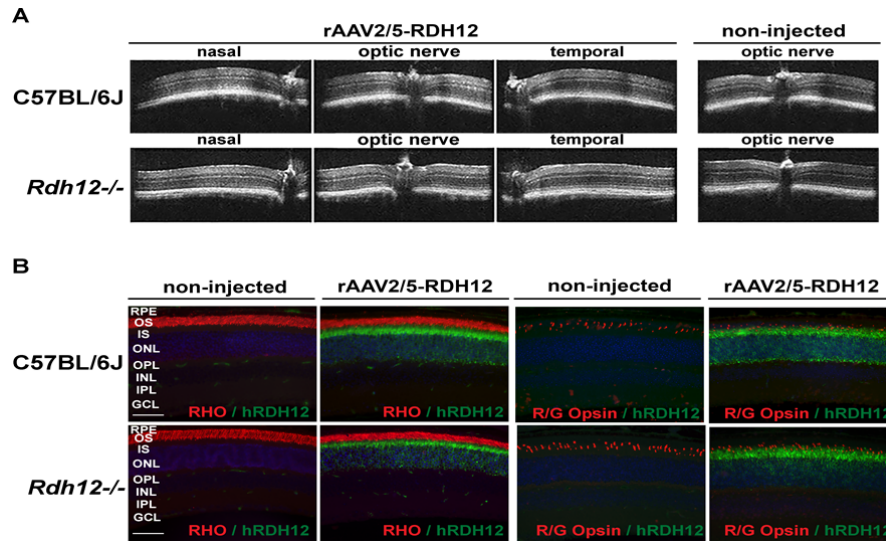
46. Wenzel A, Reme CE, Williams TP, Hafezi F, Grimm C. The Rpe65 Leu450Met variation increases retinal resistance against light-induced degeneration by slowing rhodopsin regeneration. *J Neurosci* 2001;21:53-58.
47. Aleman TS, Uyhazi KE, Serrano LW, et al. RDH12 Mutations Cause a Severe Retinal Degeneration With Relatively Spared Rod Function. *Invest Ophthalmol Vis Sci* 2018;59:5225-5236.
48. Sodi A, Caputo R, Passerini I, Bacci GM, Menchini U. Novel RDH12 sequence variations in Leber congenital amaurosis. *Journal of AAPOS : the official publication of the American Association for Pediatric Ophthalmology and Strabismus* 2010;14:349-351.
49. Chacon-Camacho OF, Jitskii S, Buentello-Volante B, Quevedo-Martinez J, Zenteno JC. Exome sequencing identifies RDH12 compound heterozygous mutations in a family with severe retinitis pigmentosa. *Gene* 2013;528:178-182.
50. Garg A, Lee W, Sengillo JD, Allikmets R, Garg K, Tsang SH. Peripapillary sparing in RDH12-associated Leber congenital amaurosis. *Ophthalmic Genet* 2017;38:575-579.
51. Fahim AT, Bouzia Z, Branham KH, et al. Detailed clinical characterisation, unique features and natural history of autosomal recessive RDH12-associated retinal degeneration. *Br J Ophthalmol* 2019.

## FIGURE LEGENDS

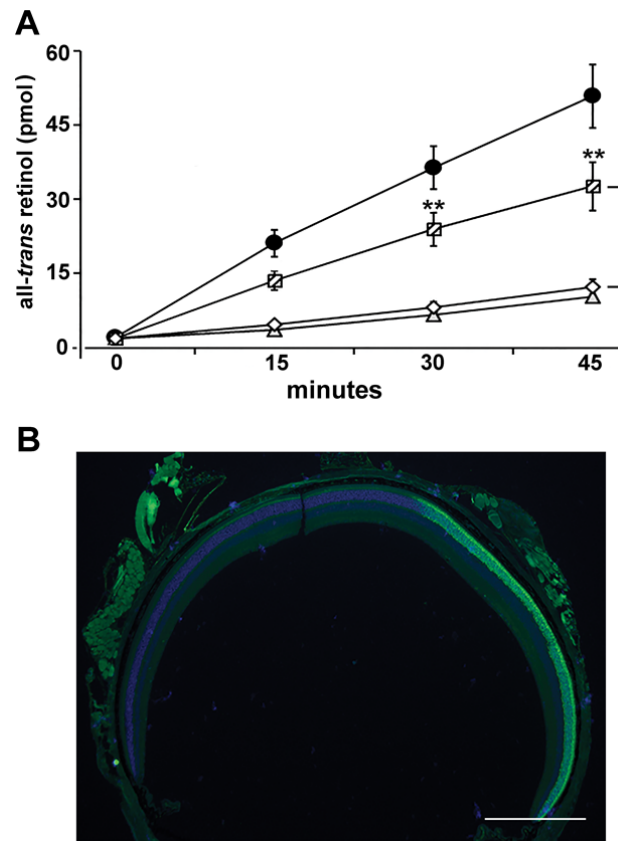


**Figure 1: Expression of human RDH12 in mice that received sub-retinal injection of rAAV2/5-hGRK1p.hRDH12.** **(A)** Schematic of pAAV-hGRK1p.hRDH12 in which a human RDH12 cDNA is cloned downstream of a human rhodopsin kinase (GRK1) promoter and in between inverted terminal repeat sequences derived from the AAV2 genome. **(B)** SYPRO™ Ruby-stained gel of purified AAV2/5 preparations showing VP1, 2 and 3 capsid proteins. Lanes: L, Biorad precision plus dual color standard; 1, AAV2/5 reference sample ( $10^{10}$  vg); 2, rAAV2/5-hGRK1p.hRDH12 ( $10^{11}$  vg). **(C, D)** RDH12 expression at 6 weeks after sub-retinal injection of rAAV2/5-hGRK1p.hRDH12 ( $1.4 \times 10^9$  vg), evaluated using antibodies specific for mouse *Rdh12* (mRdh12) or human RDH12 (hRDH12), as indicated. **(C)** Western analysis of retinal lysates from non-injected C57BL/6J mice (anti-mRdh12), rAAV2/5-hGRK1p.hRDH12-injected *Rdh12*<sup>-/-</sup> mice (anti-hRDH12), and PBS-injected *Rdh12*<sup>-/-</sup> mice (anti-hRDH12). GAPDH was a loading control. **(D)** Immunohistochemical analysis of endogenous mouse *Rdh12* (red; anti-mRdh12) shows localization to the IS, ONL, and OPL in retinal sections from C57BL/6J mice, but not in *Rdh12*<sup>-/-</sup> mice. Immunohistochemical analysis of recombinant human RDH12 (green; anti-hRDH12) resulting from injection of rAAV2/5-hGRK1p.hRDH12 shows localization to the IS, ONL, and OPL in both C57BL/6J and *Rdh12*<sup>-/-</sup> mice. Immunoreactivity in the OPL corresponds to RDH12 present in the inner most region of the photoreceptor inner segments. Dots of immunoreactivity scattered across the inner retina represent cross reactivity with blood vessels seen in non-perfused

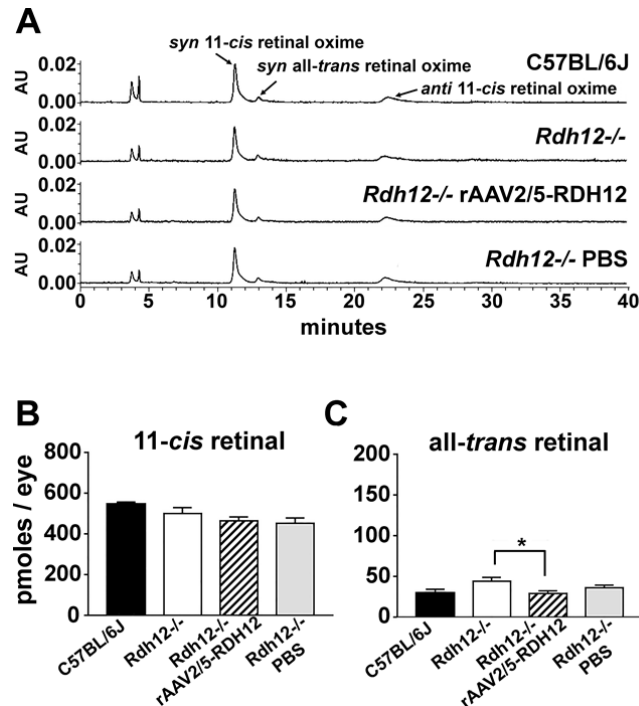
tissue with some preparations of anti-hRDH12. DAPI staining of nuclei (blue). Phase contrast images are shown to the left. Images of retina sections from non-injected mice evaluated by immunohistochemical analysis with anti-hRDH12 are shown to the right. Scale bars, 50  $\mu$ m. Abbreviations: ITR, inverted terminal repeat; hGRK1, human rhodopsin kinase promoter; SD/SA, Simian virus 40 splice donor/splice acceptor site; hRDH12, human RDH12 cDNA; polyA, Simian virus 40 polyadenylation signal; RPE, retinal pigment epithelium; OS, outer segments; IS, inner segments; ONL, outer nuclear layer; OPL, outer plexiform layer; INL, inner nuclear layer; IPL, inner plexiform layer; GCL, ganglion cell layer.



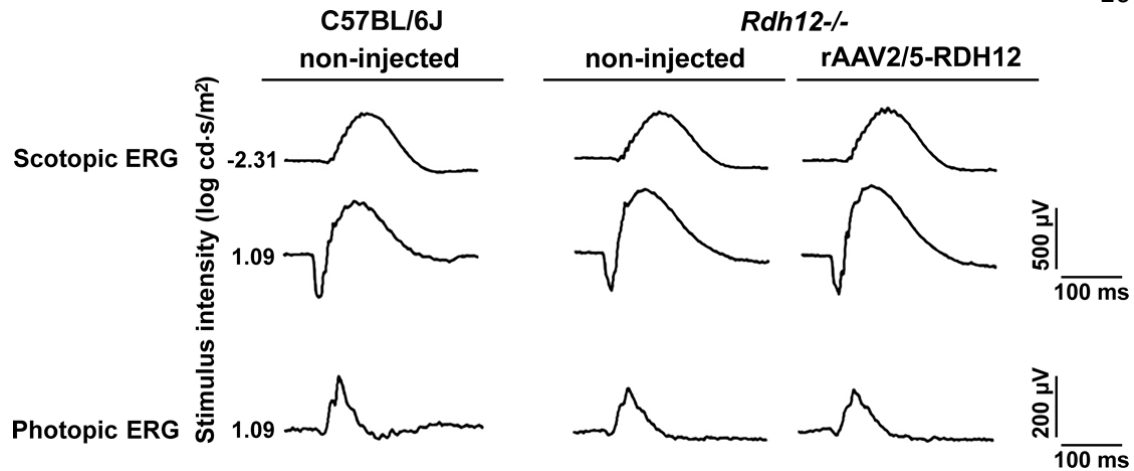
**Figure 2: Expression of human RDH12 does not perturb mouse retinal structure or visual pigment localization. (A, B)** C57BL/6J and *Rdh12*<sup>-/-</sup> mice received a sub-retinal injection of rAAV2/5-hGRK1p.hRDH12 ( $1.5 \times 10^9$  and  $1.4 \times 10^9$  vg, respectively) in one eye, and the other eye was not injected. **(A)** OCT analysis of retinal microstructure. Representative images from injected and non-injected contralateral eyes taken 6 weeks postinjection are shown. **(B)** Immunohistochemical analysis of rhodopsin and cone opsin expression in retinal sections from injected and non-injected contralateral eyes evaluated 16 weeks postinjection. Human RDH12 (green) and mouse rhodopsin (red) (left-side panels). Human RDH12 (green) and mouse red/green opsin (red) (right-side panels). DAPI staining of nuclei (blue). Scale bars, 50 μm. Abbreviations as in Figure 1.



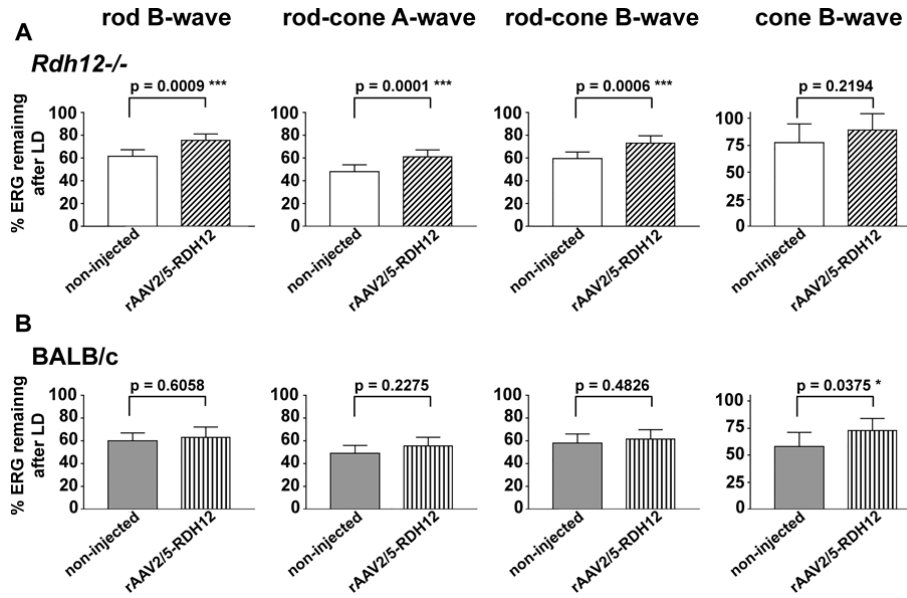
**Figure 3: rAAV2/5-hGRK1p.hRDH12 restores RDH12 activity in *Rdh12*-deficient mice. (A)** HPLC analysis of retinal reductase activity in retinas from non-injected C57BL/6J mice, and from *Rdh12*<sup>-/-</sup> mice that received a sub-retinal injection of rAAV2/5-hGRK1p.hRDH12 ( $1.3 \times 10^9$  vg) or PBS, or were non-injected. At 6 weeks postinjection, all-*trans* retinol formation was quantitated in assays of retinal homogenates containing added NADPH and all-*trans* retinol. Each data point represents the mean  $\pm$  standard error for a minimum of 5 independent experiments in which retinas from 3 to 5 mice were pooled and assayed in triplicate. ● C57BL/6J ; △ non-injected *Rdh12*<sup>-/-</sup> ; ◇ PBS-injected *Rdh12*<sup>-/-</sup> ; ◻ rAAV2/5-hGRK1p.hRDH12-injected *Rdh12*<sup>-/-</sup>. \*\*  $p < 0.01$ . **(B)** Immunohistochemical analysis of human RDH12 expression in a whole eye cross-section from an *Rdh12*<sup>-/-</sup> mouse at 16 weeks rAAV2/5-hGRK1p.hRDH12 postinjection. Scale bar, 500  $\mu$ m. Human RDH12 (green). DAPI stained nuclei (blue).



**Figure 4: rAAV2/5-hGRK1p.hRDH12 does not significantly decrease steady-state levels of 11-*cis* retinal.** HPLC analysis of retinoids in retinas from non-injected C57BL/6J mice, and from *Rdh12*<sup>-/-</sup> mice that received a sub-retinal injection of rAAV2/5-hGRK1p.hRDH12 ( $1.4 \times 10^9$  vg) or PBS, or were non-injected. At 6 weeks postinjection, following overnight dark adaptation, retinoids were extracted under dim-red light, and quantified by HPLC analysis. **(A)** Representative chromatograms from each treatment condition: peaks for *syn* 11-*cis* retinal oxime, *anti* 11-*cis* retinal oxime, and *syn* all-*trans* retinal oxime are indicated. For groups of 10-14 mice for each treatment condition, total levels of **(B)** 11-*cis* retinal and **(C)** all-*trans* retinal were quantified and plotted as the mean  $\pm$  standard error. \*  $p < 0.05$ .



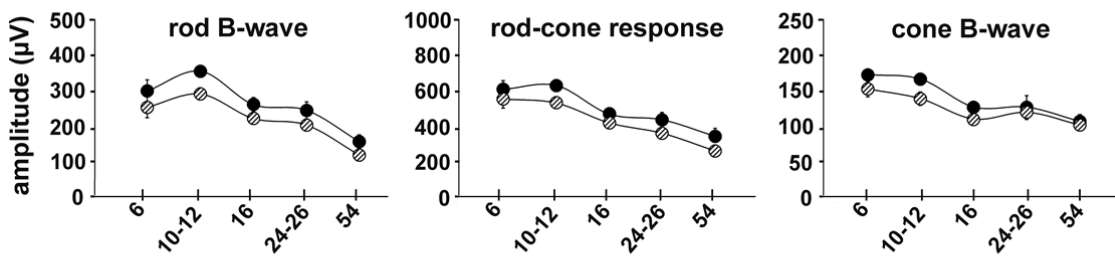
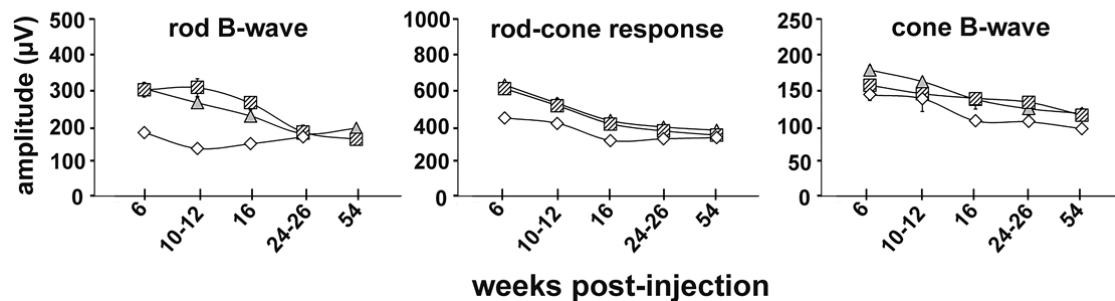
**Figure 5: rAAV2/5-hGRK1p.hRDH12 does not inhibit retinal function.** Scotopic (rod-isolated and combined rod-cone) and photopic (cone-mediated) ERG responses recorded from non-injected C57BL/6J mice, and from *Rdh12*<sup>-/-</sup> mice at 6 weeks postinjection of rAAV2/5-hGRK1p.hRDH12 ( $1.4 \times 10^9$  vg) in one eye. Representative ERGs from each treatment group are shown.



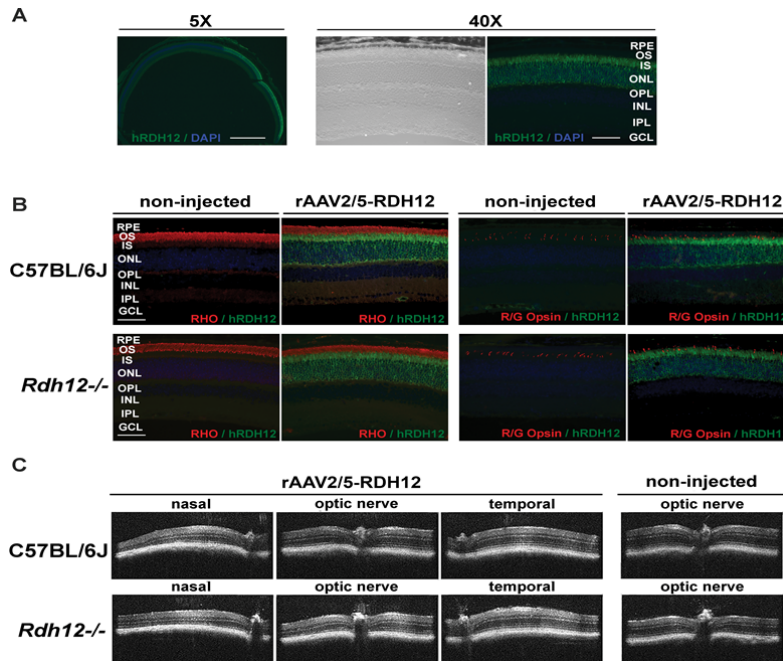
**Figure 6: rAAV2/5-hGRK1p.hRDH12 gene-replacement therapy reduces light-damage in albino *Rdh12*-deficient mice.** ERG analysis was performed, before and after exposure to 5,000 lux for 2 h, on wild-type BALB/c and albino *Rdh12*<sup>-/-</sup> mice in which one eye received a sub-retinal injection of rAAV2/5-hGRK1p.hRDH12 ( $1.4 \times 10^9$  vg), and the contralateral eye was not injected. Scotopic (rod-isolated and combined rod-cone) and photopic responses were quantified for groups of 10-13 mice. The percentage of the initial response remaining after light damage was calculated for injected and non-injected eyes. Mean outcomes  $\pm$  standard error are shown for **(A)** albino *Rdh12*<sup>-/-</sup> mice and **(B)** wild-type BALB/c mice, as well as the significance of the differences between injected and non-injected eyes calculated using two-tailed paired t-test analysis: \*\*\*  $p < 0.001$ , \*  $p < 0.05$ .

## SUPPLEMENTAL FIGURE LEGENDS

## C57BL/6J

*Rdh12*<sup>-/-</sup>

**Supplemental Figure 1: Long-term retinal function is not adversely affected by rAAV2/5-hGRK1p.hRDH12.** At times up to 54 weeks postinjection, ERG responses were measured from C57BL/6J and *Rdh12*<sup>-/-</sup> mice that received a sub-retinal injection of rAAV2/5-hGRK1p.hRDH12 ( $1.4 \times 10^9$  vg) or PBS in one eye. Scotopic responses were elicited by brief xenon white flashes from -5.8 to +1.09 log cd-s/m<sup>2</sup>. Following a 10 minute exposure to a white 32 cd/m<sup>2</sup> rod-suppressing background, light-adapted ERGs were recorded in response to 1.09 log cd-s/m<sup>2</sup> intensity flashes. ● non-injected C57BL/6J; ⊙ rAAV2/5-hGRK1p.hRDH12-injected C57BL/6J; ▲ non-injected *Rdh12*<sup>-/-</sup>; ▣ rAAV2/5-hGRK1p.hRDH12-injected *Rdh12*<sup>-/-</sup>; ◇ PBS-injected *Rdh12*<sup>-/-</sup>. Mean response amplitudes ± standard error are plotted; the error bars are obscured by the symbols in many instances.



**Supplemental Figure 2: Long-term expression of human RDH12 does not cause retinal damage in mice.** C57BL/6J and *Rdh12*<sup>-/-</sup> mice received a sub-retinal injection of rAAV2/5-hGRK1p.hRDH12 ( $1.4 \times 10^9$  vg) in one eye, and no injection in the contralateral eye. Representative images at 54 weeks postinjection are shown. **(A, B)** Immunohistochemical analysis of expression in retinal sections. **(A)** Human RDH12 (green) at low (5x) and high (40x) magnification (green). Scale bars, 500  $\mu$ m and 50  $\mu$ m, respectively. **(B)** Human RDH12 (green), mouse rhodopsin (red), and mouse red/green opsin (red). DAPI staining of nuclei (blue). Scale bars, 50  $\mu$ m. **(C)** OCT analysis of retinal microstructure in eyes that received rAAV2/5-hGRK1p.hRDH12, and in non-injected contralateral eyes.